PROC. OF JSCE,
No. 316, Dec. 1981

STUDY ON ESTIMATION OF FATIGUE STRENGTHS OF NOTCHED STEEL MEMBERS

By Chitoshi MIKI, Toshio NISHIMURA**, Hiroaki TANABE***, and Kazuhiro NISHIKAWA*****

1. INTRODUCTION

Members of steel structures have notches almost everywhere such as parts of configuration change, rivet holes, bolt holes and scallops, and fatigue cracks are often initiated with these as starting points. Consequently, clarifying the effects of notches on fatigue strength is an effective matter in considering the fatigue strengths of steel structures.

The repetitive stress-strain conditions at the root of a notch will differ depending on the magnitude of the load acting on the member and the shape of the member, but they may be broadly classified as follows:

i) The entire cross section of the member yields and plastic strains are repeated.
ii) The root of the notch yields locally and plastic strains are repeated.
iii) The root of the notch yields locally but only elastic strains are repeated due to shakedown.
iv) The root of the notch does not yield at all.

Of these cases, ii) is the one for which estimation of strains repeated at the root of the notch is complicated and often occur in structural members. The present study has evaluation of fatigue strengths under such strain conditions as its main objective, and takes up what may be classified as so-called low-cycle fatigue problems (fatigue life not more than approximately 10^5 cycles).

Regarding the effects of notches on fatigue strength, fatigue limits which mostly had been obtained by rotating bending fatigue tests, were compiled and these are being utilized in design of machinery elements using notch coefficients and notch sensitivities[1]. However, the effects of notches in low-cycle fatigue have not been studied very much since phenomena such as changes in mechanical properties of the material accompanying repetitive plastic strain are complex. Crews and Hardrath[2] measured strains at the roots of notches by the photoelastic coating method and strain gages, and studied their relations with fatigue strength. Nagai et al.[3),4)], Iida et al.[5)], and Kawamoto et al.[6)] measured strains at the roots and surroundings of notches by the Moire method, Yagi et al.[7)], by strain gages, and Nishitani et al.[8)] by metallurgical microscope, and the relations between these and fatigue strength or comparisons with the results of fatigue tests on smooth specimens were studied.

Elasto-plastic finite element analysis is effective for estimating stress-strain properties at root of notch. Okugawa and Okumura[9)] estimated the stress-strain behaviors of notched members subjected to repetitive loads from initial loadings to several cycles by finite element analysis and showed good agreement with measured values. However, to successively calculate steady-state stress-strain behaviors from the time of initial loading is extremely difficult, and it is necessary to devise an approximate estimation method. Murakami and Kusumoto[10)] carried out finite element method analysis using the curve which was obtained from gradually varying stress amplitude test of a smooth test piece as the stress-strain relationship. While, Utoguchi and Nozue[11)] used the cyclic stress range-strain range curve obtained from strain controlled fatigue tests as the stress-strain relationship to carry out finite element method analysis. Both of them considered that the strain values thus obtained were

* Member of JSCE, Dr. Eng., Associate Professor, Department of Civil Engineering, University of Tokyo
** Member of JSCE, Dr. Eng., Professor, Department of Construction Engineering, Gunma University
*** Member of JSCE, M. Eng., Engineer, Civil Engineering Design Section, Kajima Corporation
**** Member of JSCE, M. Eng., Research Engineer, Public Words Research Institute, Ministry of Construction

the strain range in steady-state during fatigue tests, and the results of fatigue tests on specimens with circumferential notches were plotted against these strain range. Iida and Koh[12] carried out finite element method analysis considering the cyclic stress-strain curve as the stress-strain relationship, and arranged the results of repeated tension fatigue tests on notched plates with strain values obtained by the analysis as strain amplitudes.

Because the stress distribution in the neighbourhood of a notch is three-dimentional condition, and because transient phenomena such as cyclic hardening and cyclic softening of steel occur under plastic strain repetition, it is fairly difficult to accurately grasp the strain behavior which has the closest relationship with initiation of fatigue cracks. In order to estimate the fatigue strength of notched members, it is necessary to examine that the appropriate srtess-strain relationship to be employed, the effect of plate thickness in the case of plate members, or how the stress ratio is to be considered. Further, the relationship between strain properties of notch root and fatigue strength has not been adequately explained by past studies.

In the present study, the steady-state strain range at the root of a notch under repetitive loading was computed by finite element method analysis taking the cyclic stress range-strain range curve as the stress-strain relationship, and the appropriateness of this estimation method was examined through comparisons with measured values. The life of each notched specimen until initiation of fatigue crack were plotted against the estimated strain range obtained by finite element analysis, and this was compared with the fatigue curve of the base material.

2. SPECIMENS AND METHOD OF TESTING

(1) Fabrication of Specimens

The steels for testing were 50 kg/mm² (500 N/mm²) class low-alloy steel (SM50A), 60 kg/mm² (600 N/mm²) class and 80 kg/mm² (800 N/mm²) class quenched and tempered high-strength steels (SM58 and HT80). The mechanical properties and chemical compositions of the steels are shown in **Table 1**. SM58 was used to compare fatigue characteristics of weld metal (WM), and heat affected zone (HAZ) with those of the base metal (BM) because the mechanical properties of quenched and tempered steel is sensitive to heat. Welding was done manually using low-hydrogen type electrodes by a single skilled welder. The mechanical properties and chemical compositions of the electrodes are shown in **Table 2**. The groove shape adopted was double V groove for complete joint penetration. Preheating temperatures were from 100 to 120°C. The penetration condition is shown in **Photo 1**.

The configurations and dimensions of specimens are shown in **Fig. 1**. For examination of the fatigue properties of the base material the hourglass type specimen (WES-162-3[15]) of a) was used. Specimens of SM58 steel were cut out from the welded plates so as to the minimum cross section were situated at BM, HAZ and WM. The axis of all specimens were made to coincide with the roll direction of the steel and these were taken from the middle portions of plate thickness. Specimen surfaces after being finished by

Table 1 Mechanical Properties and Chemical Compositions (Mill Sheet Values) of Steels Tested.

Steel	Mechanical Properties			Chemical Composition (%)										Remarks
	Yield Point (kg/mm²)	Tensile Strength (kg/mm²)	Elongation (%)	C *	Si *	Mn *	P **	S **	Cu *	Cr *	Mo *	V *	B **	
SM50A	33	51	28	16	34	130	17	18	—	—	—	—	—	Plate thickness 16 mm
SM58	59	65	35	13	26	117	17	6	—	18	—	3	—	Plate thickness 22 mm
HT80 (HW70)	84	88	31	11	27	89	11	3	24	91	32	4	1	Plate thickness 16 mm

*: (×100), **: (×1 000)
Specimens: SM50A JIS-1A, SM58 JIS-4, HT80 JIS-5

Table 2 Mechanical Properties and Chemical Compositions (Mill Sheet Values) of Welding Rods.

Welding Rod (Diam.)	Mechanical Properties			Chemical Composition (%)							Remarks
	Yield Point (kg/mm²)	Tensile Strength (kg/mm²)	Elongation (%)	C *	Mn *	Si *	P **	S **	Ni *	Mo *	
LB-62 (φ4 mm)	56.3	67.3	29	7	122	57	12	5	59	27	Used for welding first pass
LB-62 (φ5 mm)	55.3	63.9	27	8	116	54	13	9	58	24	Used for other passes

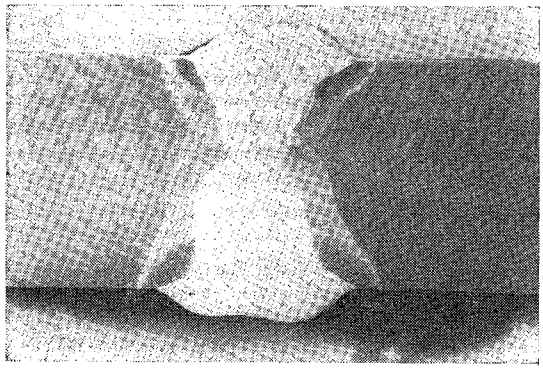

Photo 1 Penetration at Weld (SM58).

machine were polished with sandpaper of very fine grain (#1 000) until scratchs in the circumferential direction by tool were completely removed.

The influences of notches on fatigue strengths were studied using the circumferentially notched specimens of (b) and the notched specimens of (c) in **Fig. 1**. The circumferentially notched specimens of (b) were fabricated from welded plates of SM58 steel with the shapes of notches being the two kinds of semi-circle (elastic stress concentration factor $K_t=2.37$) and V-notches ($K_t=4.60$) with the roots of these notches corresponding to BM, HAZ and WM. The composition of the notch root of the each specimen was confirmed by etching test. The notched specimens of (c) were fabricated from SM50 and HT80 steels, and with the aim of model representation of notches existing in structural members, two types with side notches ($K_t=3.65$, 6.90) and two types with center notches ($K_t=2.45$, 4.55) were employed. The original plates of the tested steels were 16 mm in thickness, but surfaces were shaved 3 mm on each side to obtain testing portions of uniform quality.

(2) Method of Testing

The fatigue tests of hourglass type specimens and circumferentially notched specimens were performed using a closed loop system servo-pulsers of dynamic capacity ± 5.0 tons, and the fatigue tests of the notched specimens by a same type machine of dynamic capacity of ± 50 tons.

The fatigue tests of hourglass type specimen were carried out under strain controlled conditions applying axial loads exceeding yield stress (strain ratio $R=-1$) and load controlled conditions applying axial loads below yield stress (stress ratios $R=0$, -1). The method of the strain controlled conditions is as described in Ref. 16).

For circumferentially notched specimens, fully

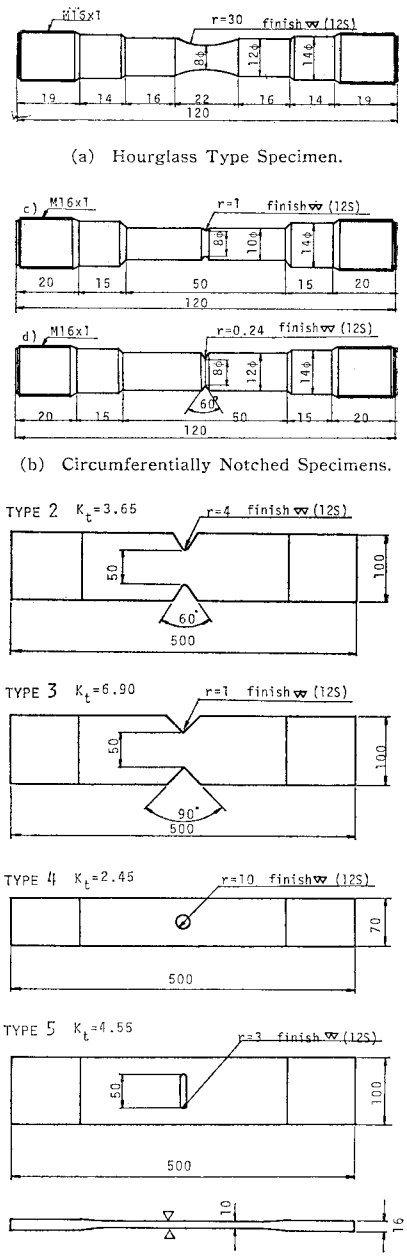

Fig. 1 Configurations and Dimensions of Specimens (Unit: mm).

reversed axial load fatigue tests were performed. The stress waveforms applied were sine waves.

The major part of tests of notched specimens were carried out under repeated tensile load with minimum load as 0, partially fluctuating load tests with stress ratio -0.5 were also performed to some extent. The stress waveform applied was a sine wave.

Strain gages were mounted at the side wall of notch roots of some of the type-2, 4, 5 notched specimens and the behaviors of strains under cyclic loading were investigated. In such case, since there was risk of gage characteristics being changed accompanying load repetitions, gages were re-pasted as suited endeavoring to make it possible for strains to be correctly measured. The strain gages used were as follows:

Side wall of notch root—gage length 0.3 mm, grid width 1.4 mm

Specimen surface notch surroundings (minimum cross section)—gage length 1.0 mm, grid width 1.5 mm, (stress concentration gage).

Observations of fatigue cracks initiated at the surface of hourglass type specimens and circumferentially notched specimens were made by trinocular microscopes ($6X-40X$). Observations of fatigue cracks in notched specimens and measurements of crack lengths were made by optical microscopes on collecting replicas from locations where initiation was foreseeable at predetermined numbers of cycles (numbers of cycles 1/10 to 1/20 of crack initiation life presumable). Further, two-stage multi-stress amplitude fatigue tests where stress amplitude were reduced by half during constant stress amplitude tests at every certain number of cycles, and initiation of fatigue cracks and the conditions of their propagation were clarified from beach marks remaining at fracture surfaces.

3. FATIGUE PROPERTIES OF BASE MATERIAL

(1) Strain Range-Fatigue Life Curve Diagram

Fig. 2 shows the strain range-fatigue life curves of SM50 and HT80 base metals obtained from strain controlled fatigue tests and load controlled fatigue tests. Of these, the results of strain controlled fatigue tests have been reported in Ref. 16. The plastic strain range (ϵ_{pr}) and the elastic strain range (ϵ_{er}) were calculated using hysteresis loops at the $N_f/2$ number of cycles (N_f: failure life), while the total strain range (ϵ_{tr}) was $\epsilon_{pr}+\epsilon_{er}$. The $\epsilon_{er}(=\epsilon_{tr})$ in the load controlled fatigue

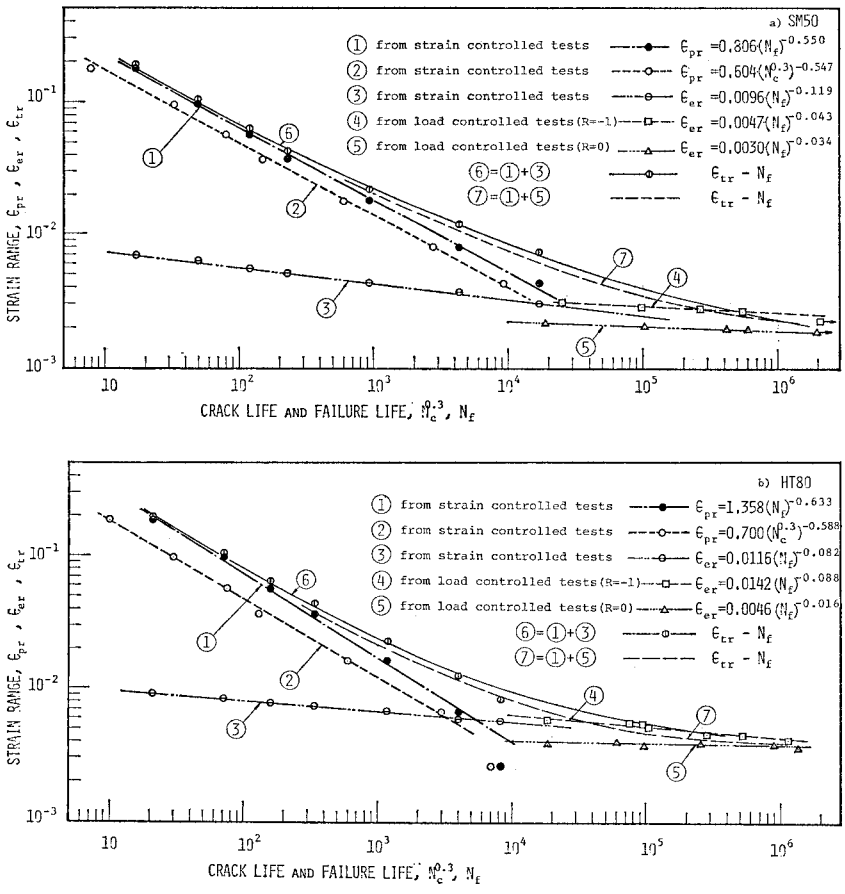

Fig. 2 Strain Range-Fatigue Life of SM50 and HT80 Base Metal.

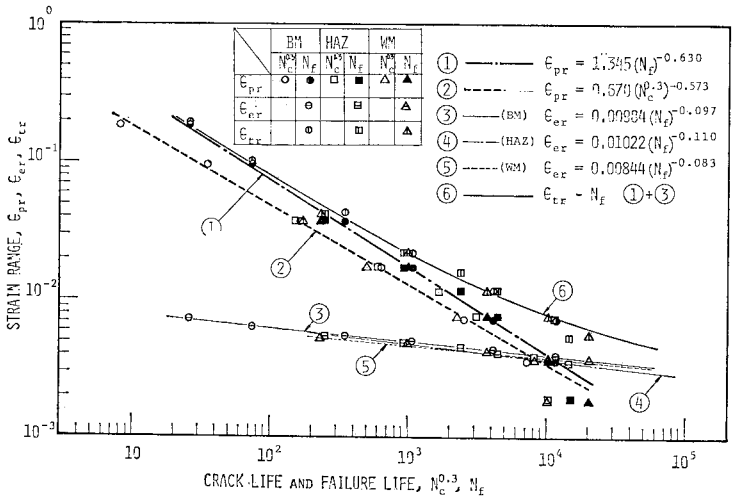

Fig. 3 Strain Range-Fatigue Life or SM58 Weld Components (BM, HAZ, WM).

tests is the true stress range divided by the modulus of elasticity. The crack initiation life ($N_c^{0.3}$) is the number of cycles when a fatigue crack of length of 0.3 mm is formed at the surface of the specimen. The $\epsilon_{pr}-N_f$ (line ①), $\epsilon_{pr}-N_c^{0.3}$ (line ②) and $\epsilon_{er}-N_f$ (line ③) obtained from strain controlled fatigue tests of SM50 and HT 80 indicate good linearities in log-log scale. The $\epsilon_{er}-N_f$ relation (line ④) obtained from load controlled fatigue tests also indicates linearity.

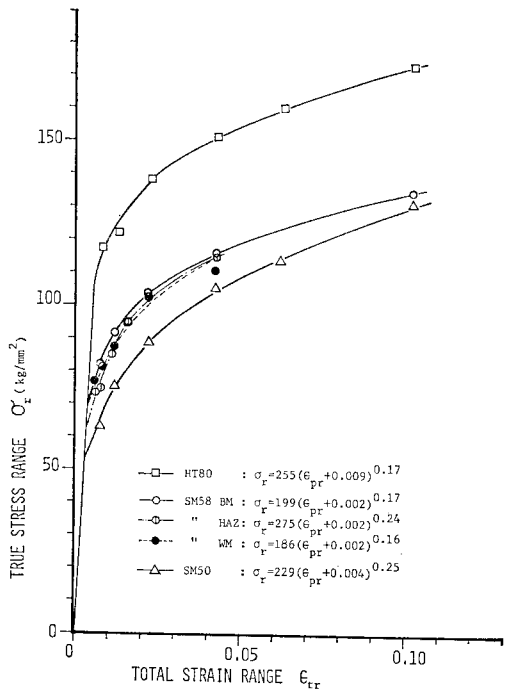

Fig. 4 Cyclic Stress Range-Strain Range Curves.

However, the line ④ obtained from the load controlled test of $R=-1$ is not on the extension of line ③. Therefore, it is slightly difficult to set a fatigue curve for the high-cycle fatigue range applying the curve obtained from the strain controlled test in the low-cycle fatigue range.

Fig. 3 shows the results of strain controlled fatigue tests of specimens of WM, HAZ, BM of SM58 steel. Since hardly any difference due to composition can be recognized in the relations of $\epsilon_{pr}-N_f$ and $\epsilon_{pr}-N_c^{0.3}$ in the figure, the relations of $\epsilon_{pr}-N_f$ and $\epsilon_{pr}-N_c^{0.3}$ were respectively indicated by single straight lines.

(2) Cyclic Stress Range-Strain Range Curve

The cyclic stress range-strain range curve was obtained by a continuous plots of the stress range on the ordinate and the strain range on the abscissa under steady-state of each strain controlled test. The stress and strain ranges were calculated from the hysteresis loops of the number of cycles $N_f/2$. The cyclic stress range-strain range curves obtained in this manner are indicated in **Fig. 4**. These curves are indicated in the figure obtaining the relationship when $\sigma_r=C(\epsilon_{pr}+a)^n$ is set[17] by the method of least squares.

4. ESTIMATION OF STEADY-STATE CYCLIC STRAIN RANGE OF NOTCH ROOT

(1) Cyclic Stress-Strain Properties

Fig. 5 gives the measured values of axial strains at initial tensile loading and at the 10th cycle at the middle of the plate thickness of the side wall of the notch root of the Type 2 notched specimen (SM50), and the gradual changes in

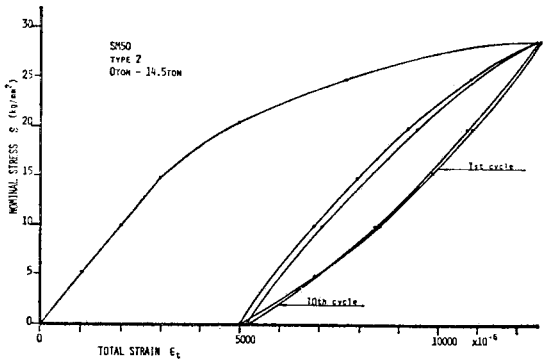

Fig. 5 Measured Strain at Notch Root.

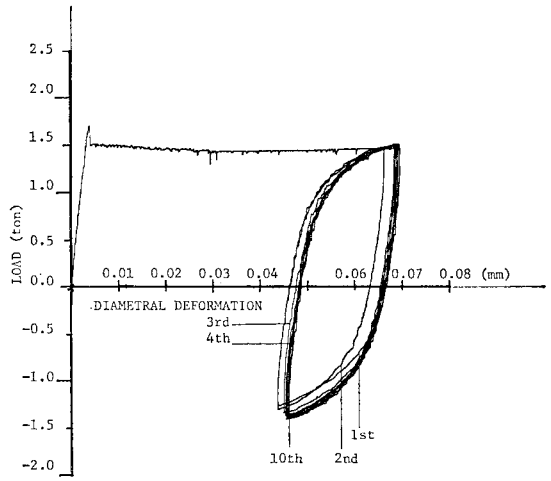

Fig. 6 Hysteresis Loops of Load-Diametral Deformation Obtained by the Strain Reproduction at Notch Root.

both average strain and strain amplitudes with repetitions of load are indicated. The hysteresis loops of load and diametral displacement in **Fig. 6** was obtained by the test that reproduced the measured values of strain shown in **Fig. 5** on an hourglass type specimen from initial loading to the 10th cycle. In spite of the fact that zero to tensile loads are repeated on the notched specimens, the roots of notches are in partially reversed stress states, and a trend gradually approaching a completely reversed stress state is recognized with increased repetitions of loading.

Because zones where plastic strains are repeated locally at roots of notches are restrained by the surrounding elastic zones, their stress-strain properties can be considered as strain controlled conditions. Further, in strain controlled fatigue tests with mean strain of hourglass specimen, the average stress which introduced by mean strain gradually disappears with repetitions of strain, and becomes a completely reversed stress condition at a steady state[16]. Consequently, it is thought that notch roots become of completely reversed stress condition at steady states. From the above, the stress ratio of the nominal stress is unrelated to fatigue crack initiation life in case plastic strains are repeated locally at roots of notches, and this was confirmed in **Fig. 14**.

(2) Elasto-plastic Analysis by the Finite Element Method

Based on the study in **(1)** above and the fact that the influence of average strain on the shape of the cyclic stress-strain curve is of a negligible degree[16], the steady-state stress distribution at the neighborhood of the notch root in case plastic strains are repeated locally may be represented in model form as in **Fig. 7**. That is, at the root of a notch, regardless of stress ratio, the stress-strain at maximum load will be a hysteresis loop tip location on the tension side, and the stress-strain at minimum load that on the compression side. The shapes of the loops are the same as the steady-state hysteresis loops of strain controlled fatigue tests of the base materials. Consequently, it is thought suitable for the strain range of steady-state at notch roots to be obtained by elasto-plastic finite element method analysis with the cyclic stress range-strain range curve as the stress-strain relationship.

Finite element method analysis were made by methods based on the strain increment theory proposed by Yamada[17),18)] and others. Judgements of yielding were made using the conditions of Mises.

When a notched plate specimen is to be analyzed as a two-dimensional problem, the effect of

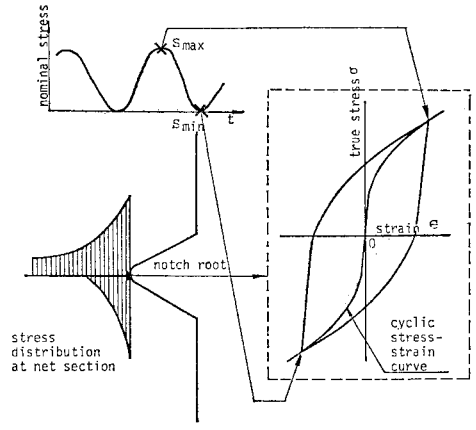

Fig. 7 Model of Steady-State Stress Distribution at Notch Root.

thickness of the plate will be a problem[19]. The thicknesses of the notched specimens in the present study were all 10 mm, and since there were some fairly sharp notches with notch root radius of 1 mm, analysis were made for all types of specimens based on plane stress assumption and plane strain assumption. Circumferentially notched specimens were analyzed as axially symmetric problems.

Fig. 8 shows the relations between nominal stress ranges (S_r) of HT80 Type 2 and Type 4 notched specimens and axial strain range (ϵ_{yr}) at notch root obtained from analysis. The strain ranges measured using strain gages at the middles of the side wall at notch roots at 50 to 70% of N_c cycles (see **5.(1)**) in fatigue tests of various specimens are also shown in **Fig. 8**.

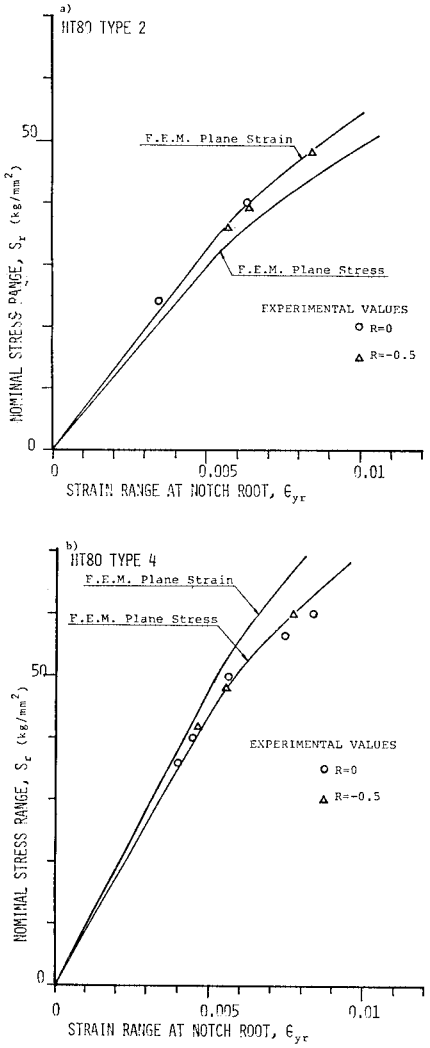

Fig. 8 Nominal Stress Range and Axial Strain Range at Notch Root.

Regardless of stress ratios, the measured values are close to analytical results assuming plane strain in case of Type 2 specimens and analytical results assuming plane stress in case of Type 4 specimens. The results with SM50 specimens are similar. When plate thicknesses are equal, the stress conditions at the middles of the side wall at the notch roots approach plane strain conditions the sharper the notches, and in the present study the notched specimens with the smallest elastic stress concentration factor was Type 4 specimen, followed by Type 2 specimen. Therefore, in estimation of strain ranges at these locations, it is thought suitable for analysis based on plane stress assumptions to be made for Type 4 notched specimen, and those based on plane strain assumptions to be made for other specimen types.

Fig. 9 is an example of comparisons of analytical and measured values for axial strain range distribution with minimum cross-section of notched specimens, and the two show fairly good agreement.

Based on the above, it is possible to estimate with good accuracy the steady-state cyclic strain range at notch root through finite element method

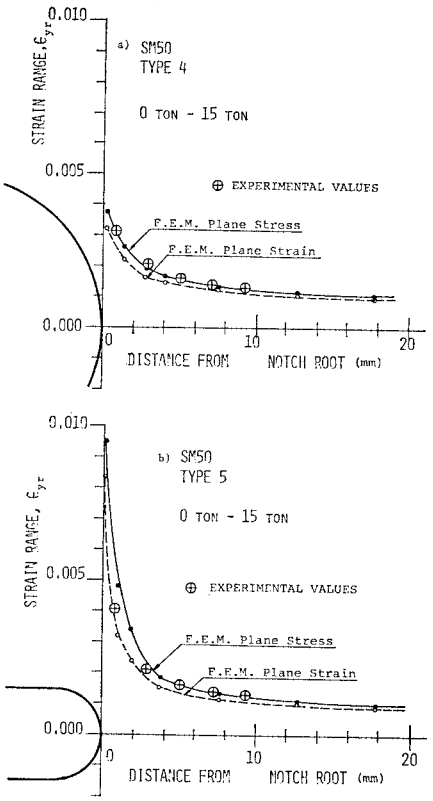

Fig. 9 Strain Range Distribution at Minimum Cross Section of Notched Specimen.

analysis taking the cyclic stress range-strain range curve as the stress-strain relationship.

(3) Strain Range Concentration Factor

To indicate the degree of concentration of stress and strain at notch root under elasto-plastic state, stress concentration factor (K_σ) and strain concentration factor (K_ε) are used. Neuber[13] has proposed Eq. (1) and Stowell, Hardrath and Ohman[14] proposed Eq. (2) as methods of estimating these from elastic stress concentration factor (K_t).

$$\left.\begin{aligned} &K_\sigma \cdot K_\varepsilon = K_t^2 \\ &\text{Rewritten, this will be} \\ &K_\sigma = K_t\left(\frac{E_N}{E_S}\right)^{1/2}, \quad K_\varepsilon = K_t\left(\frac{E_S}{E_N}\right)^{1/2} \end{aligned}\right\} \quad \cdots\cdots(1)$$

$$\left.\begin{aligned} &K_\sigma = 1+(K_t-1)\frac{E_N}{E_S} \\ &K_\varepsilon = (K_t-1)+\frac{E_S}{E_N} \end{aligned}\right\} \quad \cdots\cdots(2)$$

where

E_S: secant modulus corresponding to the average stress on the net section.

E_N: secant modulus corresponding to the local stress at the notch root.

It would be convenient, if, by replacing the stress-strain relationships for these equations by cyclic stress range-strain range curves the steady-state strain range concentration factor (ΔK_ε) could be estimated. **Fig. 10** compares ΔK_ε of HT80 notched specimens calculated by Eq. (1) and Eq. (2), and $\Delta K\varepsilon$ calculated from results of finite element method analysis. The values of ΔK_ε by Eq. (1) are larger than ΔK_ε by the finite element method for all types of notched specimens, whereas values of ΔK_ε by Eq. (2), excepting those for Type 3 specimens of sharpest notches, are in relatively good agreement with the values of ΔK_ε by the finite element method. The results with SM50 specimens are similar. Consequently, when elastic stress concentration factor is known, and it is lower than about 4.5, by using the cyclic stress range-strain range curve in the Stowell-Hardrath-Ohman equation, it will be possible to estimate the approximate value of the strain range regularly repeated at the notch root.

5. FATIGUE STRENGTH OF NOTCHED MEMBER

(1) Fatigue Crack Initiation Properties and Crack Initiation Life

The crack initiation life (N_c) of a circumferentially notched specimen was taken to be the number of cycles at which fatigue crack were discovered at the bottom surface of a notch. Fatigue cracks were discovered at surface length of 0.2 to 2.0 mm in all specimens. Because fatigue cracks rapidly extend around the entire circumference after initiation, this N_c was almost equal to $N_c^{0.3}$ in fatigue tests of base materials.

In notched specimens, initiation and propagation properties of the fatigue cracks in the early stage differ according to shapes of notches and the magnitude of acting loads. **Photo 2** shows

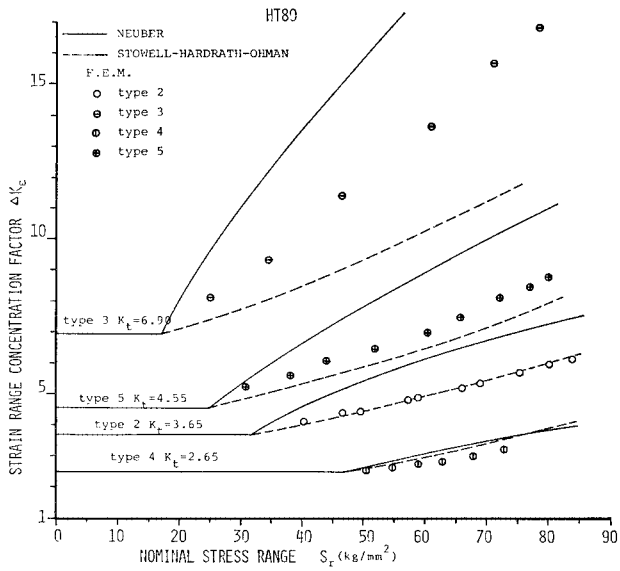

Fig. 10 Strain Range Concentration Factor.

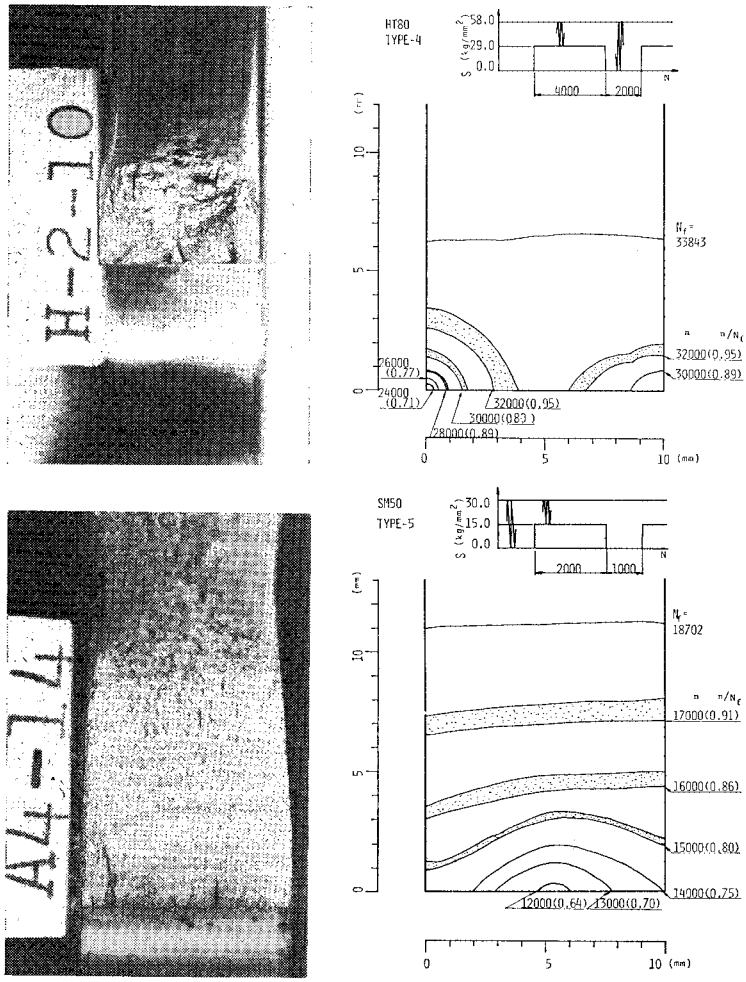

Photo 2 Beach Marks at Fatigue Fracture Surfaces of Notched Specimens.

the examples of beach marks of fracture surfaces obtained in two-stage multi-stress amplitude fatigue tests. Since one beach mark is formed for each single block halving the stress amplitude after initiation of fatigue crack, it is possible to find from them the locations of fatigue crack initiation and changes in shape accompanying growth. The numerical values given the beach marks observation diagrams are numbers of cycles (n) ignoring the cycles halving the stress amplitude, and its ratio (n/N_f) to the failure life (N_f).

With Type-4 notched specimens, according to observations of these beach marks, fatigue cracks are initiated both from the edges of notches and from the side walls at notch roots of notches. This trend agrees with the fact that the measured strain range at the middle of the side wall at notch root is close to the analytical value for the plane stress assumption. That is to say the strains at the side wall of the notch root are roughly uniform in the direction of plate thickness. With notched specimens of other types, fatigue cracks were initiated from the vicinities of middles of the side walls of notch roots.

It is very difficult to find minute fatigue cracks at the side walls of notch roots. Consequently, the crack initiation life (N_c) of a notched specimen was taken to be the number of cycles at which a fatigue crack of length of 0.5 mm was discovered at the surface of specimen. Therefore, when a fatigue crack was initiated from middle of the side wall of notch root, as is clearly seen in **Photo 2**, this N_c is a value attained after a number of cycles of loading subsequent to crack initiation.

(2) Relationship between Stress Range and Fatigue Life

In **Fig. 11** crack initiation lives (N_c) and failure lives (N_f) of circumferentially notched

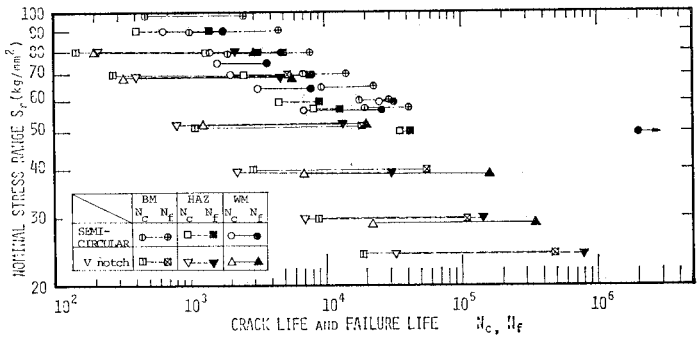

Fig. 11 Nominal Stress Range vs. Fatigue Life of Notched Specimens.

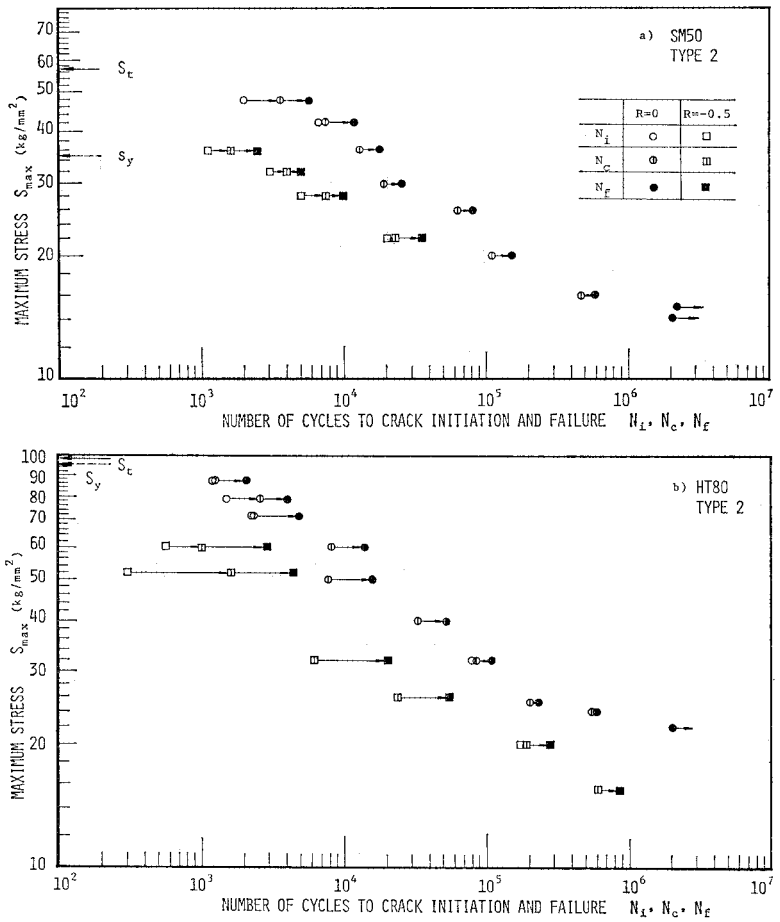

Fig. 12 Maximum Nominal Stress vs. Fatigue Life of Notched Specimens.

specimens were plotted against nominal stress range in log-log scale. The number of cycles from N_c to N_f of V-notched specimens are very long, while there are much differences between N_c of semi-circularly notched specimens and N_c of V-notched specimens at the same S_r. As for fatigue lives of WM, HAZ and BM, differences between them were not much recognized other than BM in semi-circular notch specimens being of longer life than the other two components.

Fig. 12 shows the relationships of N_c and N_f and maximum nominal stress (S_{max}) of notched specimens in log-log scale. For specimens on which fatigue crack initiation was recognized at

Table 3 Fatigue Strengths of Notched Specimens at Specified Life.

Specimen	Material	Fatigue Strength N_f (kg/mm²)				Fatigue Strength N_c (kg/mm²)			
		5×10^3	1×10^4	1×10^5	1×10^6	5×10^3	1×10^4	1×10^5	1×10^6
Type 2	SM 50	49	43	22	15	44	39	20	—
〃	HT 80	70	60	32	22	65	50	28	—
Type 3	SM 50	37	30	17	9.5	26	22	12	—
〃	HT 80	56	47	20	12	32	27	18	—
Type 4	SM 50	50	48	30	26	—	46	29	—
〃	HT 80	88	76	44	36	84	72	42	—
Type 5	SM 50	42	36	20	13.6	36	32	19	—
〃	HT 80	62	50	26	17	50	42	23	—

side walls of notch roots, the number of cycles N_i at times of recognition have been indicated. The S_y and S_t on the ordinate of this figure are the nominal stress at general yielding and tensile strength, respectively, in static tension tests of each two notched specimens. **Table 3** shows the fatigue strengths at specified life (averaged value) of notched specimens obtained from repeated tensile load fatigue tests. For specimens of the same steel, fatigue strength is lower the shaper the notch. While for specimens of the same type, fatigue strength of HT80 steel was considerably higher than it of SM50 steel in the short-life range, with the two becoming closer together with longer life, and in addition, sharper the notch.

(3) Relationship between Strain Range and Fatigue Life

Fig. 13 is the result of plotting the crack initiation lives (N_c) of circumferentially notched specimens against steady-state plastic strain ranges (ϵ_{pr}) of notch roots obtained by finite element method analysis in log-log scale. These strain ranges are equivalent strains not axial strains. Equivalent strain would be more suitable than axial strain in considering the three-dimensional nature of strains at locations of fatigue crack initiation. The solid line in the figure is the $\epsilon_{pr}-N_c^{0.3}$ relation (line ② in **Fig. 3**) obtained from strain controlled fatigue tests. The all test values of semi-circular notch specimens and of V-notched specimens are more or less gathered together with this one straight line at the center. Based on this, it was clarified that when the plastic strain hystereses at fatigue crack initiation points are equal, fatigue cracks are initiated at the same number of cycles whether or not there are notches and irrespective of notch shapes.

Fig. 14 indicates the relationships of crack initiation lives (N_c) and steady-state plastic strain ranges (ϵ_{pr}) at notch roots of the various SM50 and HT80 notched specimens in a manner similar to **Fig. 13**. The broken line and the dot-and-dash line in the figure are the $\epsilon_{pr}-N_c^{0.3}$ and $\epsilon_{pr}-N_f$ relations (lines ①, ② in **Fig. 2**), respectively, obtained from strain controlled fatigue tests of base metals. The various experimental values of notched specimens are close to the $\epsilon_{pr}-N_f$ line of the base material regardless of notch shapes. Those which do not coincide with the $\epsilon_{pr}-N_c^{0.3}$ line of the base metals

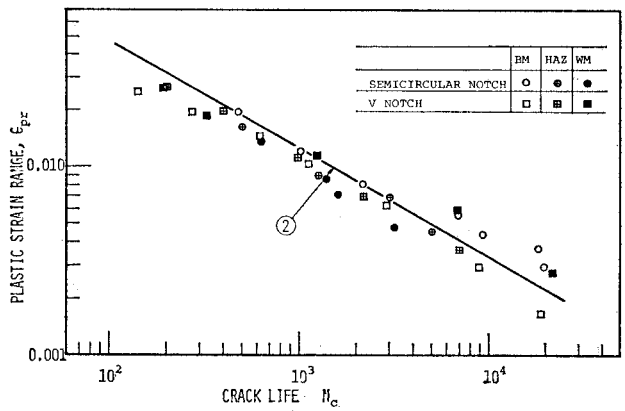

Fig. 13 Plastic Strain Range vs. Crack Initiation Life of Circumferentially Notched Specimens.

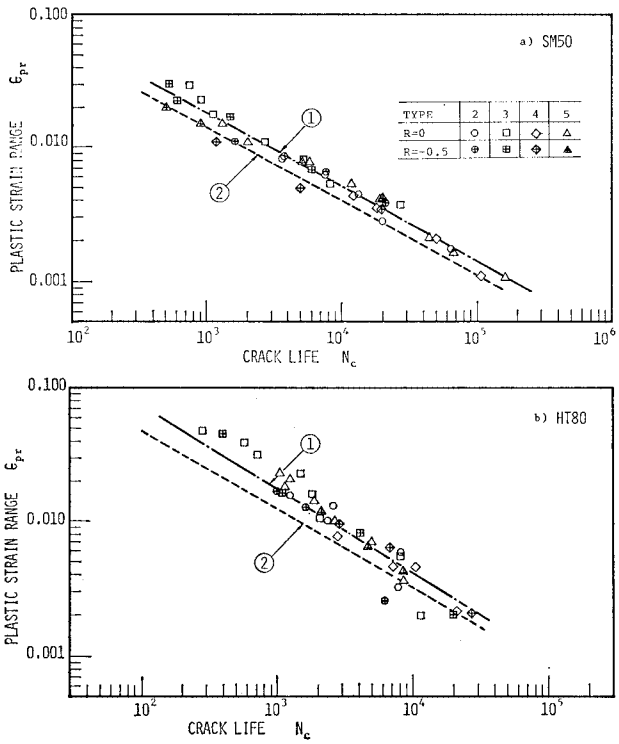

Fig. 14 Plastic Strain Range vs. Crack Initiation Life of Notched Specimens.

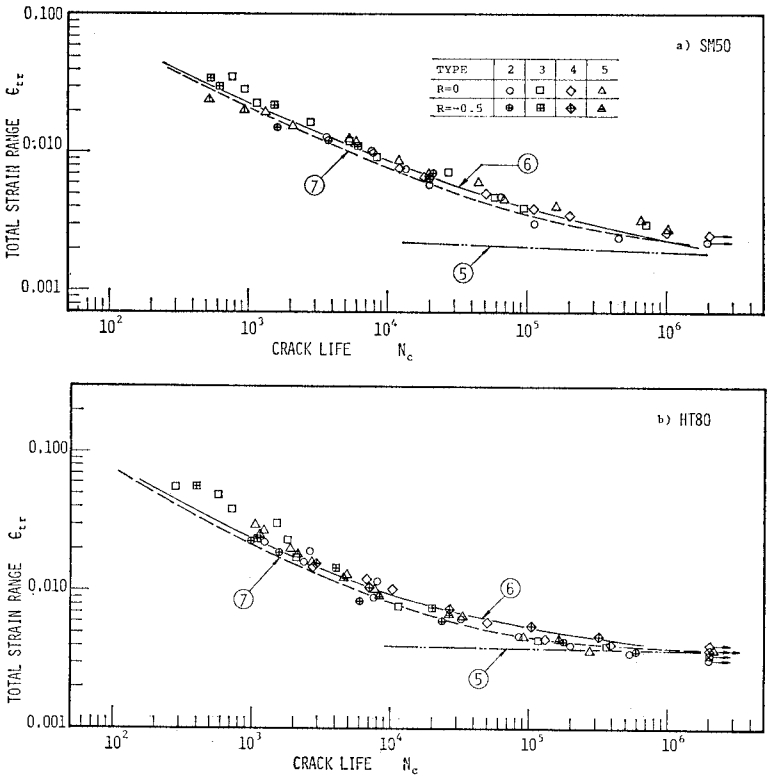

Fig. 15 Total Strain Range vs. Crack Initiation Life of Notched Specimens.

are those based on the definition of N_c of notched specimens. When N_c of notched specimens are based on initiation of minute cracks at the side walls of notch roots (see **Fig. 12**), it is anticipated that similar results to those for circumferential notch specimens will be obtained. The influences of stress ratio disappeared almost completely both SM 50 and HT80.

Fig. 15 expresses N_c of notched specimens as logarithms against the estimated total strain range $\epsilon_{tr}(=\epsilon_{pr}+\epsilon_{er})$, with the straight line and the curves in the figure indicating ⑤ and ⑥, ⑦ of **Fig. 2**. In the high-cycle fatigue range, the experimental values are on fairly high strength side compared with the $\epsilon_{er}-N_c$ line (⑤) obtained from fatigue tests of base metals. In contrast, with HT80 specimens, the experimental values and the $\epsilon_{er}-N_c$ line (⑤) roughly agree at around 10^6 cycles. The $\epsilon_{tr}-N_f$ curve (⑦) obtained by adding together the $\epsilon_{pr}-N_f$ line from strain controlled fatigue tests in the low-cycle fatigue range and the $\epsilon_{er}-N_f$ line from load controlled fatigue tests in the high-cycle fatigue range is in fairly good agreement with the relations of ϵ_{tr} and N_c of notched specimens in broad life ranges for both SM50 and HT80. This $\epsilon_{tr}-N_f$ curve, as indicated in **Fig. 2**, is not in agreement with experimental values of base metals in the high-cycle fatigue range and the physical significances are not distinct, but it may be said to be an effective relation for predicting the approximate fatigue strengths of notched members in a broad life range.

6. CONCLUSIONS

The major results of the present study are summarized as follows:

(1) The strain range-fatigue life curve diagrams of the SM50 and HT80 base metals were set from strain controlled fatigue tests in the low-cycle fatigue range, and from load controlled fatigue tests in the high cycle fatigue range. The $\epsilon_{er}-N_f$ relation obtained from load controlled tests did not necessarily fall on the extension of the $\epsilon_{er}-N_f$ relation obtained from strain controlled tests.

(2) There were almost no differences of $\epsilon_{pr}-N_c^{0.3}$ and $\epsilon_{pr}-N_f$ relations between BM, HAZ and WM of SM58.

(3) In case that the root of the notch yields locally and plastic strains are repeated, the average stress at the notch root disappears with repetitions of load, and at steady states, a completely reversed stress state is brought about regardless of the nominal stress ratio. Consequently, the strain range of steady-state at the roots of notches can be estimated by elasto-plastic finite element method analysis with the cyclic stress range-strain range curve as the stress-strain relationship.

(4) The steady-state strain ranges measured at middles of side wall at notch roots of notched specimens, regardless of nominal stress ratios, agreed with finite element method results for plane stress assumption for Type-4 specimens ($K_t=2.45$), and plane strain assumption for Type-2 specimens ($K_t=3.65$). The analytical and measured results of axial strain range distributions with minimum cross sections roughly coincided.

(5) The N_c of a circumferentially notched specimen was taken to be the number of cycles at which fatigue crack of 0.2 to 2.0 mm length was discovered at the bottom surface of a notch. The relations between ϵ_{pr} of steady-state at notch root and N_c agreed with the $\epsilon_{pr}-N_c^{0.3}$ line of base materials.

(6) The N_c of a notched specimen was taken to be the number of cycles at which a fatigue crack of length of 0.5 mm was discovered at the surface of specimen. The relation between ϵ_{pr} of steady-state at notch root and N_c agreed with the $\epsilon_{pr}-N_f$ line of the base materials.

(7) From these results, it was clarified that regardless of type of steel and weld composition, when the plastic strain hystereses at fatigue crack locations are the same, fatigue cracks are initiated at identical number of cycles regardless of whether or not there are notches. In this case, the nominal stress ratio has no relation with crack initiation life.

ACKNOWLEDGEMENTS

A part of these studies was carried out under a 1977 Ministry of Education Scientific Research Grant, while another was conducted as a part of the activities of the "Working Group on High- and Low-Cycle Fatigue, Metals Subcommittee, Japan Material Committee" organized in the Japan Testing Center for Construction Materials. The studies were made and the data compiled with guidance and advice from Professor Morihisa Fujimoto and Associate Professor Yutaka Yoshida of Tokyo Institute of Technology and Professor Kunihiro Iida of the University of Tokyo. The experimentation work was done aided greatly by Technical Official Masayuki Tsurumaki of the Civil Engineering Department, Tokyo Institute of Technology, and student Tohru Natori (now with Yokogawa Bridge Works, Ltd.). The authors wish to express their sincerest gratitude to all those mentioned above.

REFERENCES

1) The Japan Society of Mechanical Engineers: Design Data for Fatigue Strength of Metals, 1961. 5 (in Japanese).
2) Crews, J. H. Jr., H. F. Hardrath: A Study of Cyclic Plastic Stresses at Notch Root, Experimental Mechanics, pp. 313~329, 1966. 6.
3) Nagai, K., A. Otsuka and K. Okawa: Behaviors of Plastic Strain on Steels Subjected to Low-Cycle Pulsating Tension, Journal of the Society of Naval Architects in Japan, No. 124, pp. 355~374, 1968. 12 (in Japanese).
4) Nagai, K., M. Iwata and S. Nishimura: Effect of Notch on Behaviors of Plastic Strain on Steels Subjected to Low Cycle Pulsating Tension, Journal of the Society of Naval Architects in Japan, No. 127, pp. 207~214, 1970. 6 (in Japanese).
5) Ando, Y., K. Iida and I. Soya: Initiation and Propagation of a Crack and Cyclic Behavior of Strain in Low Cycle Fatigue, Journal of the Society of Naval Architects in Japan, No. 128, pp. 343~357, 1970. 12 (in Japanese).
6) Kawamoto, M., H. Namiki, Y. Toya and T. Yasuda: Strain Distribution and Fatigue Strength of Notched Specimen under Low Cycle Fatigue Test, Transactions of Japan Society of Mechanical Engineers, Vol. 40, No. 337, pp. 2478~2452, 1974. 9 (in Japanese).
7) Yagi, J., Y. Tomita, S. Fujiwara and Y. Toyama: Studies on the Low Cycle Fatigue of Steels (3rd Report), Journal of the Society of Naval Architects in Japan, No. 135, pp. 365~377, 1974. 6 (in Japanese).
8) Nishitani, H. and M. Kage: Strain Concentration or Notched Specimens in Low Cycle Fatigue (Push-Pull and Torsion), Transactions of Japan Society of Mechanical Engineers, Vol. 41, No. 344, pp. 1044~1051, 1975. 4 (in Japanese).
9) Okugawa, A. and T. Okumura: Elastic-Plastic Behaviors of Notched Member under Repetitive Loading, Proceedings of 7th Conference on Matrix Methods of Structural Analysis, Japan Society of Steel Construction, pp. 127~131 (in Japanese).
10) Murakami, Y. and S. Kusumoto: Notch Effect in Low-Cycle Fatigue (1st Report, Low-Cycle Fatigue Strength of 0.48% Carbon Steel under Constant Load Amplitude), Transactions of Japan Society of Mechanical Engineers, Vol. 39, No. 319, pp. 780~789, 1973. 2 (in Japanese).
11) Udoguchi, T. and Y. Nozue: Notch Effect in Low Cycle Fatigue (2nd Report), Transactions of the Japan Society of Mechanical Engineers, Vol. 41, No. 344, pp. 1052~1061, 1975. 4 (in Japanese).
12) Iida, K. and Y. Kho: Fatigue Strength Reduction Factor of Mild and High Strength Steels. Journal of the Society of Naval Architects in Japan, No. 141, pp. 257~267, 1977. 6 (in Japanese).
13) Neuber, H.: Theory of Stress Concentration for Shear Strained Prismatical Bodies with Arbitrary Nonlinear Stress-Strain Law, Transactions of ASME., Journal of Applied Mechanics, pp. 544~550, 1961. 12.
14) Hardrath H. F. and L. Ohman: A Study of Elastic and Plastic Stress Concentration Factors Due to Notches and Fillets in Flat Plates, NACA Report 1117, 1951.
15) WES 162-1970, Testing Method of Strain Cycling Fatigue of Metallic Material for Welded Assemblies (in Japanese).
16) Nishimura, T. and C. Miki: Strain Controlled Low Cycle Fatigue Behavior of Structural Steels, Proceedings of the Japan Society of Civil Engineers, No. 289, pp. 29~44, 1979. 9 (in Japanese).
17) Yamada, Y.: Matrix Method in Material Mechanics, Baifu-kan, 1970. 11. 30 (in Japanese).
18) Yamada, Y.: Matrix Method in Plasticity and Visco-Elasticity, Baifu-kan, 1972. 5. 20 (in Japanese).
19) Nishitani, H. and Y. Murakami: Effects of Shapes, Thickness and Stress Type on Strain Concentration, Transactions of the Japan Society of Mechanical Engineers, No. 750-1, pp. 135~146, 1975. 4 (in Japanese).

(Received July 26, 1979)